HIGH-EFFICIENCY MICROMORPH SILICON SOLAR CELLS WITH IN-SITU INTERMEDIATE REFLECTOR DEPOSITED ON VARIOUS ROUGH LPCVD ZNO

D. Dominé, P. Buehlmann, J. Bailat*, A. Billet, A. Feltrin, and C. Ballif
University of Neuchâtel, Institute of Microtechnology, Photovoltaics and Thin Film Laboratory
Breguet 2, CH-2000 Neuchâtel, Switzerland
Phone: (+)41 32 718 3312; Fax: (+)41 32 718 3201; e-mail: didier.domine@unine.ch
*Now at: Oerlikon Solar-Lab S.A., Puits-Godets 6a, CH-2000 Neuchâtel, Switzerland

ABSTRACT: Light management using intermediate reflector layers (IRL) and advanced front transparent conductive oxide (TCO) morphologies is needed to rise the short-circuit current density (J_{sc}) of micromorph tandem solar cells above 14 mA/cm^2. For micromorph cells deposited on surface-textured ZnO layers grown by low-pressure chemical vapour deposition (LPCVD), we study the interplay between the front TCO layer and the IRL and its impact on fill factor and current matching conditions. The key role of the angular distribution of the light scattered by the front LPCVD ZnO layer is highlighted. A micromorph cell with 11.1% stabilized conversion efficiency is demonstrated. By increasing the bottom cell thickness and adding an antireflection coating, a J_{sc} value of 13.8 mA/cm^2 is achieved. This remarkably high J_{sc} yields 13.3% initial conversion efficiency.
Keywords: Thin Film Solar cell, ZnO, Tandem

1 INTRODUCTION

High conversion efficiency for "micromorph" tandem solar cells requires a dedicated light management and optimized growth conditions of the microcrystalline silicon (µc-Si:H) material for the bottom cell absorber.

Light management is performed using rough and highly transparent conductive oxide (TCO) layers as front electrodes. Moreover, to minimize the light-induced degradation, the thickness of the a-Si:H absorber should not exceed 300 nm, typically. This constraint considerably limits the short-circuit current density (J_{sc}) photogenerated in the top cell and, hence, the efficiency of the whole device. Thus, an intermediate reflecting layer (IRL) between the individual cells must be introduced to increase J_{sc} in the a-Si:H absorber of the top cell [1-5].

The electrical characteristics of the bottom cell are affected by the microstructure of the intrinsic µc-Si:H material. This microstructure depends on the plasma deposition conditions and shows that cracks and voids formation induced by the surface morphology of the substrate can occur during the growth [6, 7]. At IMT Neuchâtel, this issue is solved by a change of the surface morphology of the front ZnO layer from V- to U-shaped valleys with a plasma post-treatment [6].

In this paper, we first analyze the light scattering properties of nano-textured transparent conductive oxide (TCO) layers used as front electrodes for micromorph cells deposited in the superstrate (p-i-n) configuration. Photocurrents in individual state-of-the-art cells with a Si oxide based IRL (SOIR) [5] are then compared for front TCOs with different surface morphologies. The interplay of the front TCO and IRL on the fill-factor (FF) and open-circuit voltage (V_{oc}) of the micromorph device is also discussed. Finally, we present the latest results obtained at IMT for state-of-the-art micromorph tandem cells.

2 EXPERIMENTAL

2.1 Front TCO

The front TCO layers used in this study are as grown surface textured ZnO films with two different doping levels obtained by low-pressure chemical vapour deposition (LPCVD) on AF45 borosilicate glass substrates from Schott. The thickness of the resulting layers is adjusted to obtain a sheet resistance of about 10 Ω/sq. The root mean square value of their surface roughness (σ_{rms}) is determined by atomic force microscopy. These characteristics, summarized in Tables I and II for the two sets of front ZnO layers used in this study, depend on the thickness of the layers and on the duration of the plasma post-treatment applied to their surface. By increasing the post-treatment time, the surface changes from V- to U- shaped morphology and σ_{rms} decreases.

Table I: Thickness d, carrier concentration N [8], and surface roughness σ_{rms} for the 1st set of front ZnO layers (Type-A, -B and -C). Type B: no post-treatment.

Type of front ZnO	A	B	C
d (µm)	1.9	4.8	4.8
N (cm^{-3})	1.4x10^{20}	4x10^{19}	4x10^{19}
σ_{rms} (nm)	66	178	165

Table II: Same as Table I for the 2nd set of type-C (lightly doped) front ZnO layers.

Type of front ZnO	C1	C2	C3	C4
d (µm)	4.8	4.8	4.8	4.8
N (cm^{-3})	4x10^{19}	4x10^{19}	4x10^{19}	4x10^{19}
σ_{rms} (nm)	122	160	169	175

Note that the type-B ZnO (without post-treatment), whose sharp V-shape structures prevent good electrical properties of the device, is presented only for haze measurements comparisons. The low doping level used for deposition of the thick, large-grain, ZnO layers (type-B and -C) provides high transparency in the near infrared (NIR) spectral range because of reduced free carrier absorption (FCA) [8].

The diffuse transmittance in-air of the different TCO layers, when light is normally incident to the glass side, is investigated by means of their haze factor H_T and by angular resolved scattering (ARS) measurements. $H_T=T_{dif}/T_{tot}$ is calculated from total and diffuse optical

transmittance measurements (T_{tot} and T_{dif}) carried out with a Perkin-Elmer photo-spectrometer equipped with an integration-sphere. The experimental H_T is then compared with the prediction of the scalar scattering theory [9]. ARS is performed with a laser beam (633 nm) and a rotating photo-detector. The intensity measured at a scattering angle θ with respect to the direction of the incident laser beam is integrated over the azimuthal angle φ, considering an isotropic scattering over φ. This provides the transmitted intensity per unit of solid angle scattered at the angle θ [10, 11].

2.2 Micromorph solar cells

P-i-n micromorph cells and SOIR layers were deposited by very-high frequency plasma enhanced chemical vapour deposition (VHF-PECVD) [5]. The top a-Si:H cells of the tandems presented in the first part of this paper were deposited in a KAI-S deposition reactor from OC Oerlikon. The SOIR layers and the bottom μc-Si:H cells were deposited in a laboratory scale dual chamber deposition system. One chamber is dedicated to the deposition of the SOIR and doped silicon layers whereas the intrinsic silicon layers are deposited in the other chamber. The VHF-PECVD process of the state-of-the-art micromorph cells was fully completed in this dual-chamber deposition system.

The last cell presented in this paper was deposited on AF45 glass plates with one side covered with a wide band anti-reflection (AR) coating from Schott. A measurement of the reflectance of the AR coated glass (not shown here) indicates that the reflectivity at the air-glass interface is smaller than 1.2% in the 400–970 nm spectral range. In agreement with this result, comparing two micromorph cells co-deposited on AF45 glass plates with and without AR coating, a relative increase of 3% has been measured for the sum of the J_{sc} values of the individual cells for the device deposited on the glass with this AR coating.

The back contact of the cells consists of a LPCVD ZnO layer covered with a dielectric back reflector [12]. The cell area (~1.2 cm^2) is defined by SF_6 plasma etching.

2.3 Characterization of the cells

The external quantum efficiencies (EQE) of the top and bottom cells (EQE_{top} and EQE_{bot}) are measured under red and blue bias-light illumination, respectively. Short-circuit current densities for top and bottom cells ($J_{sc,top}$ and $J_{sc,bot}$) are calculated from the EQE curves, by integrating, over the wavelength range, the product of EQE times the spectral density of the photon flux of AM1.5g solar spectrum. The current density-voltage (J-V) curves are measured using a dual lamp sun simulator (Wacom) in standard test conditions (25°C, AM1.5g spectrum, 100 mW/cm^2) and normalized with the J_{sc} value deduced from the EQE measurements.

3 RESULTS

3.1 Light scattering properties of the front ZnO layers

The experimental haze factors H_T are plotted in Fig. 1 as a function of the wavelength λ of the transmitted light for the type-A, -B and -C front ZnO layers. It has been shown by Zeman et al. for Asahi U-type SnO_2:F layers and by Stiebig et al. for sputtered-etched ZnO layers, that the experimental haze of nano-textured TCO layers measured in air can be related to their surface roughness σ_{rms} by the scalar scattering theory [9], providing adjustment of two fitting parameters [13, 10]. With our LPCVD ZnO layers, we applied this fitting procedure to determine the actual H_T at the internal front ZnO/Si interface in our micromorph cells [14].

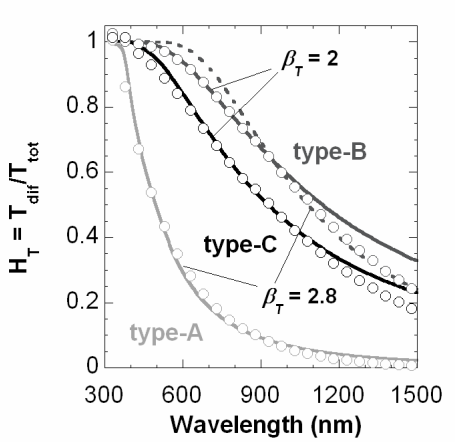

Figure 1: Experimental (symbols) and calculated (lines) haze for transmission in air through type-A, -B and -C front ZnO layers. The values of the fitting parameter β_T used for the calculation are also shown (see [14]).

The results of this calculation for the type-A and type-C front ZnO layers are plotted in Fig. 2(a). The spectral dependence of H_T at the internal ZnO/Si interface indicates that a ratio larger than 65% and 95% of the light with λ < 900 nm would be diffused by the type-A and type-C front ZnO, respectively. For λ < 700 nm this ratio increases to 85% and 100%, respectively.

Angular distribution profiles (normalized to their maximum values [11]) of the diffuse light (λ = 633 nm) transmitted in air through type-A and type-C ZnO layers are plotted in Fig. 2(b). This figure shows a narrower angular distribution for the light scattered by the type-C ZnO layer, with the most probable scattering angle equal to 15°. This value is significantly smaller than with the type-A ZnO (~40°).

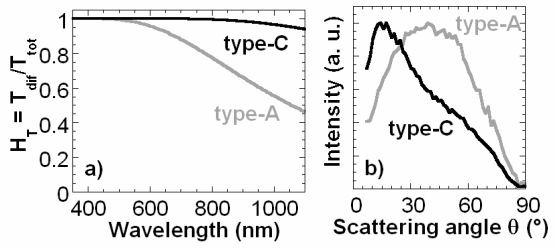

Figure 2: a) Calculated haze in transmission at the ZnO/Si internal interface for type-A and type-C front ZnO layers. b) Experimental angular distribution profiles of light (λ = 633 nm) diffused and transmitted in air by these TCO layers.

3.2 Optical interplay between the front ZnO and the IRL

EQEs of micromorph tandems deposited on type-A and type-C ZnO layers, with top cell, SOIR, and bottom cell thicknesses of 290 nm, 150 nm, and 3.0 μm, respectively, are plotted in Fig. 3. The sum of the J_{sc} values of the individual cells is increased by 7% from

25.0 to 26.8 mA/cm^2 when the tandem is deposited on the lightly doped, large grain, thick ZnO layer. This is mainly produced by a relative gain in EQE in the red and NIR parts of the spectrum. However, $J_{sc,top}$ is smaller for the micromorph cell deposited on this thicker ZnO layer. This drawback will be discussed in section 4, on the basis of the following comparison.

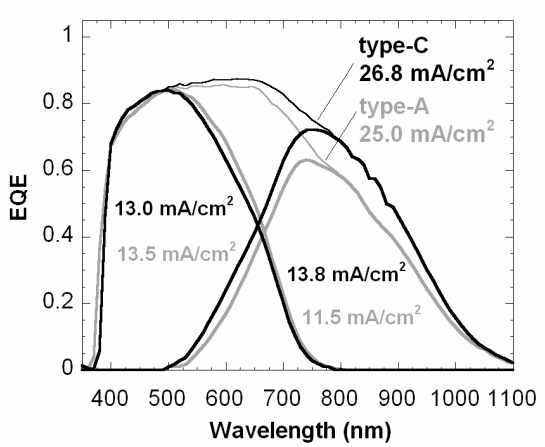

Figure 3: EQEs of micromorph cells with 150 nm thick SOIR layers deposited on type-A and type-C front ZnO.

To explain why $J_{sc,top}$ is smaller when the type-C ZnO layer with larger feature size is used as front TCO, we deposited four micromorph cells. Two cells were deposited with the insertion of a 150 nm thick SOIR layer and two cells were deposited without IRL. The deposition of these two types of device was carried out on type-A and type-C front ZnO layers. The EQE curves of these micromorph cells are plotted in Fig. 4. The striking point is that, for the two devices without IRL, the EQE_{top} curves are almost identical. However the gain in $J_{sc,top}$ ($\Delta J_{sc,top}$) obtained by insertion of the IRL is larger when the tandem is deposited on the type-A ZnO layer with smaller feature size (2.6 instead of 2.1 mA/cm^2).

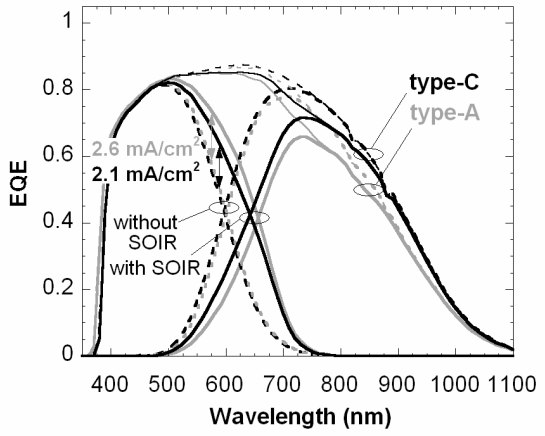

Figure 4: EQEs of micromorph cells on type-A and type-C front ZnO with/without a 150 nm thick SOIR.

3.3 Influences of the front TCO and IRL on the electrical properties of the device

The 2nd set of type-C, lightly doped, front ZnO layers (described in Table II) with different post-treatment durations was used for deposition of micromorph cells without and with a SOIR layer with different thicknesses.

Figures 5(a) and 5(c) illustrate the influence of the surface roughness of the front ZnO on the V_{oc} and FF of micromorph cells without and with a 70 nm thick SOIR layer. Note that the same PECVD deposition conditions were used, and no specific recipe improvement was implemented that could compensate in part the observed losses for FF and V_{oc}. Fig. 5(b) and 5(d) illustrate the change of V_{oc} and FF when SOIR layers of increasing thicknesses are introduced in the device.

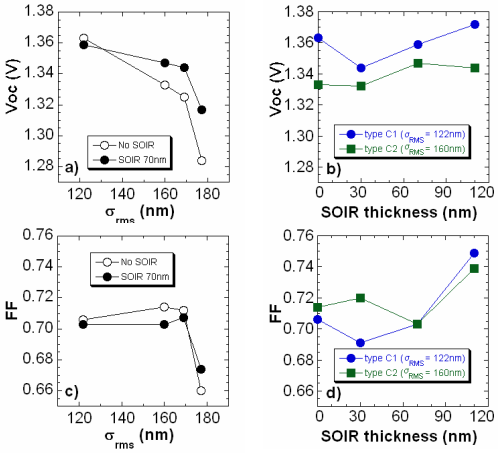

Figure 5: Dependence of V_{oc} and FF (a, c) on the surface roughness (i.e. on the post-treatment time) and (b, d) on the SOIR thickness (0 nm stands for "no SOIR layer") for type-C ZnO layers described in Table II.

The results indicate that the V_{oc} drastically decreases when σ_{rms} increases (80 mV for a 55 nm increase of σ_{rms} for the cell without SOIR) but is not influenced by the presence of the SOIR layer (no trend in Fig. 5(b)). In both cases, optimums values of σ_{rms} (i. e. optimums post-treatment times) maximize the FF (Fig. 5(c)). Fig. 5(d) indicates that, when the thickness of the SOIR layers increases, the FF value of the micromorph cells suddenly increases from about 70% to 74-75%.

The influence of the SOIR thickness on $J_{sc,top}$ and $J_{sc,bot}$ is plotted in Fig. 6. The overall loss is illustrated in the inset where the average of $J_{sc,top}$ and $J_{sc,bot}$, ($J_{sum}/2$), which corresponds to the maximum J_{sc} achievable for a current matched tandem, shows a decreasing trend when the thickness of the SOIR layer increases.

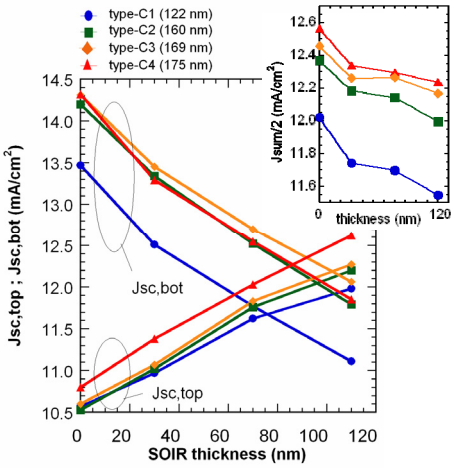

Figure 6: Dependence of $J_{sc,top}$ and $J_{sc,bot}$ on the thickness of the SOIR layer (0 nm stands for "no SOIR layer"), for micromorph cells deposited on front ZnO layers of types C1 to C4 listed in Table II. The inset shows the dependence of the average of $J_{sc,bot}$ and $J_{sc,top}$.

3.4 Micromorph cell optimization

Further optimization of our state-of-the-art micromorph device consists in choosing the best post-treatment for the lightly doped front ZnO in terms of high V_{oc} and good $J_{sc,bot}$ values and, for a given 300 nm thick top cell, in possibly adapting the thicknesses of the SOIR layer and bottom absorber to obtain a bottom-limited tandem with J_{sc} close to 13 mA/cm^2. The J-V characteristics of our best light-soaked micromorph cell in the initial state and after 1000 h of light-soaking at 50 °C are plotted in Fig. 7. It was deposited on AF45 glass plates (without AR coating) covered by a type-C2 front ZnO layer. The bottom absorber and the SOIR layer thicknesses are 3.0 µm and 150 nm, respectively, providing a bottom-limited tandem ($J_{sc,top}$=13.3 mA/cm^2) with a J_{sc} value of 12.7 mA/cm^2. The initial conversion efficiency of this cell was 12.6%. After light-soaking it stabilized to 11.1%.

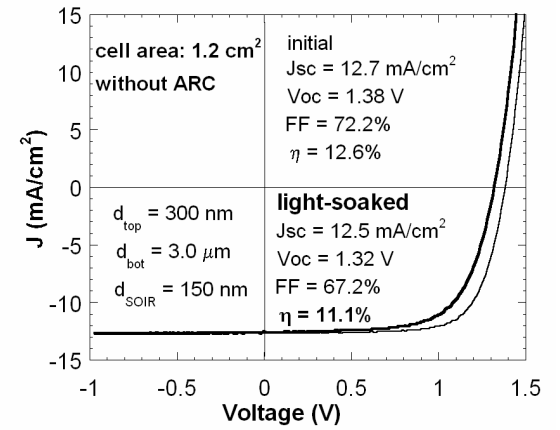

Figure 7: a) J-V curves of a micromorph cell deposited on a lightly doped, large grain, thick LPCVD ZnO layer in the initial state and after 1000 h of light soaking.

To reach initial conversion efficiencies close to 14% a further increase of J_{sc} towards 14 mA/cm^2 is needed. We therefore deposited our device on AF45 glass plates covered with the broadband AR coating from Schott. Together with an increase of the bottom cell thickness to 3.5 µm, this permitted an increase of the sum of the J_{sc} of the component cells from 26.0 mA/cm^2 to 27.7 mA/cm^2 (+6.5%). The current matching was obtained with a top cell thickness increased to 340 nm. The J-V and EQE curves of the resultant micromorph cell are plotted in Fig. 8. This tandem is slightly top limited with a remarkably high value of 13.8 mA/cm^2 for J_{sc} ($J_{sc,bot}$=13.9 mA/cm^2) and yields an initial conversion efficiency of 13.3% (V_{oc}=1.36 V, FF=70.8%).

4 DISCUSSION

4.1 Light scattering properties of the front ZnO layers

Assuming that ARS in air is relevant to predict the ZnO/Si internal interface behaviour [15], the broader angular distribution for the type-A front ZnO (Fig. 2(b)) offsets the slightly lower H_T value at the ZnO/Si interface for λ < 700 nm (Fig. 2(a)). This would explain why this less diffusive type-A ZnO is actually more suited for light trapping in a-Si:H single junction solar cells than large feature size front ZnO layers, as observed in a previous work for the 550-700 nm spectral range [4].

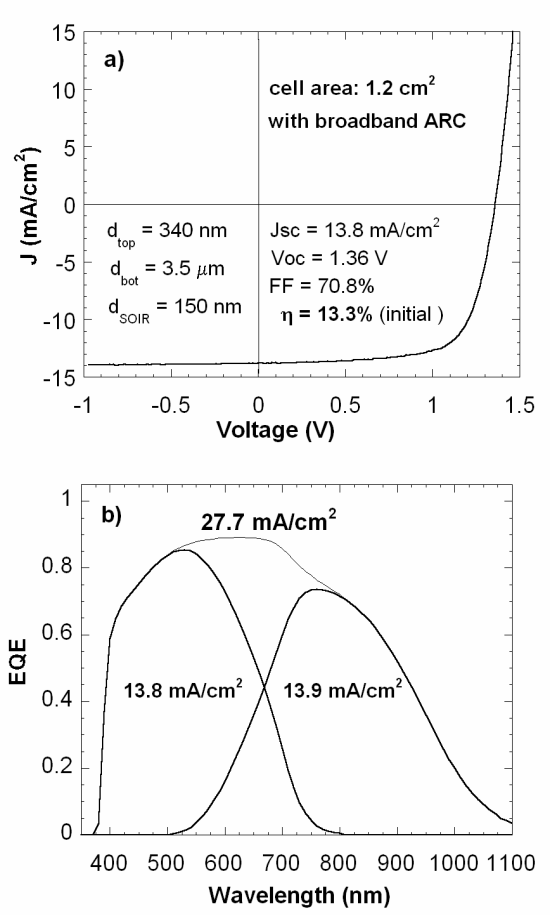

Figure 8: a) J-V curve of IMT's most recent micromorph cell deposited on a glass substrate with antireflection coating (ARC). b) EQE curves of the top and bottom cells of the same micromorph cell as in a).

4.2 Optical interplay between the front TCO and the IRL

The gain in EQE in the red and NIR parts of the spectrum for micromorph cells deposited on type-C ZnO is the consequence of the lower FCA and of the larger H_T for long wavelengths of the lightly doped and thick ZnO layers.

The striking point in the comparison of EQE curves plotted in Fig. 4 is that the EQE_{top} curves for the two devices without IRL are almost identical, despite of the very different light scattering properties measured in air (see Figs. 1 and 2(b)). We suggest the following explanation. When no IRL is inserted, light in the 550-700 nm spectral range, which is not absorbed in the top cell during the first pass, travels only once through the micromorph cell because of absorption in the thick bottom cell. This makes ineffective a possibly better light scattering capability of the front TCO in this wavelength range, because even if the critical angle of total internal reflection is reached, no light trapping will be promoted in the top cell. Therefore, for micromorph cells without IRL, light absorption in the top cell is not strongly linked to differences in the surface morphology of the different front TCO layers used in this study. Conversely, the improvement, reported in Figs. 3 and 4, of EQE_{top} in the 550-700 nm spectral range when a micromorph cell with IRL is deposited onto a ZnO layer with small feature size is accounted for by the sufficient H_T (>85%) for wavelengths shorter than 700 nm combined with a

broader angular distribution of the transmitted light scattered at this ZnO/Si interface. This enhances the light trapping promoted by the IRL in the top cell and, in turn, produces the improvement of the IRL effectiveness observed in Fig. 4.

A change of the optical reflection coefficient at the ZnO/Si interface by means of index grading, as described by the effective media approximation, takes place in the considered optical system [16]. However this index grading seems to be similar for the range of TCO surface morphologies studied here and is, hence, not included in this discussion about EQE_{top}

Note that, when an IRL is inserted, losses due to an increased total reflectance of the cell occur, as indicated by the sum of EQE_{top} and EQE_{bot} curves in Fig. 4 and by the decrease of $J_{sum}/2$ in Fig. 6.

4.3 Influences of the front TCO and IRL on the electrical properties of the device

The drastic decrease observed for V_{oc} when σ_{rms} increases (i.e. when the duration of the post-treatment of the front ZnO layer is reduced) can be related to a decrease of the V_{oc} of the individual cells of the tandem [4, 6]. For the behaviour of V_{oc} with the insertion of SOIR layers with different thicknesses, no influence can be deduced from Fig. 5(b).

The complicated behaviour of FF with the variation of σ_{rms} in Fig. 5(c) is produced by competing influences of electrical quality for the bottom µc-Si:H cell and of current matching in the tandem. Indeed, when σ_{rms} decreases with increasing post-treatment time of the front ZnO, the FF tends to be enhanced by the improved quality of the µc-Si:H material whereas it tends to be decreased when the current mismatch in the tandem decreases (type-C2 with σ_{rms}=160 nm compared to type-C1 with σ_{rms}=122 nm in Fig. 6).

Likewise, we suggest that the dramatic increase of FF observed in Fig. 5(d) with the thicker SOIR layers is caused by the current mismatch in the tandems going from top-limited to bottom-limited conditions (see J_{sc} values in Fig. 6).

4.4 Micromorph cell optimization

After light-soaking, the relative reduction of the performance of the bottom limited micromorph cell with a top cell thickness of 300 nm is 12%. Since micromorph cells with stable V_{oc} under light-induced degradation have been demonstrated [2], the relative decrease of 4% for the V_{oc} observed in this study should be avoidable. It is not fully understood yet and will require further investigations.

Note that for the top limited micromorph cell with a 13.3% initial efficiency, we have to take care, due to the increased thickness of the a-Si:H absorber (340 nm), to an expected light induced degradation larger than 12%.

The remarkably high J_{sc} value (13.8 mA/cm^2) achieved for this tandem demonstrates, however, the excellent collection efficiency of the carriers photogenerated in our relatively thick (3.5 µm) intrinsic µc-Si:H absorber. This result gets us a step closer to obtain J_{sc} values above 14 mA/cm^2, a prerequisite towards 14% micromorph cells.

5 CONCLUSIONS

In summary, we showed that an intermediate reflector layer is essential in micromorph cells to take fully advantage of the light scattering capabilities of front TCO layers in the 550-700 nm spectral range. We demonstrated a gain in $J_{sc,top}$ of 2.6 mA/cm^2 with a SOIR layer deposited *in-situ*. This gain is comparable to previous results with an *ex-situ* ZnO layer [4]. The gain is slightly larger for micromorph cells deposited on front ZnO layer with small features size because of the broader angular distribution of the light scattered by this diffuser. However, when lightly doped, thick front ZnO layers with large feature size are used as front TCOs, higher $J_{sc,bot}$ values are achieved. This is due to the low FCA and large haze in the NIR of these TCOs. With a 3.0 µm thick µc-Si:H absorber and without any AR coating, $J_{sc,top}+J_{sc,bot}$=26.8 mA/cm^2 has been obtained.

This study also highlights a complicated interplay between morphology of the front TCO and thickness of the SOIR layer in determining FF value and current matching conditions in micromorph cells. Post-treatment for the front ZnO allowed us to optimize these parameters and the best device (1.2 cm^2 and no AR coating) is a bottom limited micromorph cell with 11.1% stabilized conversion efficiency.

By increasing the bottom cell thickness to 3.5 µm and using glass substrates with a broadband AR coating, a J_{sc} value of 13.8 mA/cm^2 is achieved. This remarkably high current density yields 13.3% initial conversion efficiency and makes an important contribution in paving the road towards 14% micromorph cells.

ACKNOWLEDGMENTS

This work was supported by the Swiss Federal Energy Office (OFEN) (project number 101191) and by the EU (Athlet Project, contract 019670).

[1] D. Fischer et al., 25th IEEE PVSC , 1996, p. 1053.
[2] J. Meier et al., 3rd WCPEC, 2003, p. 2801.
[3] K. Yamamoto et al., Prog. Photovoltaics 13 (2005) 645.
[4] D. Dominé et al., 4th WCPEC, 2006, p. 1465.
[5] P. Buehlmann et al., Appl. Phys. Lett. 91 (2007) 143505.
[6] J. Bailat et al., 4th WCPEC, 2006, p. 1533.
[7] M. Python et al., J. Non-Cryst. Sol 354 (2008) 2258.
[8] J. Steinhauser et al., Appl. Phys. Lett. 90 (2007) 142107.
[9] C. K. Carniglia, Opt. Eng. 18 (1979) 104.
[10] H. Stiebig et al., 16th EUPVSEC, 2000, p. 549.
[11] M. Schulte et al., 22nd EUPVSEC, 2007, p. 2190.
[12] J. Meier et al., 31st IEEE PVSC, 2005, p. 1464.
[13] M. Zeman et al., J. Appl. Phys. 88 (2000) 6436.
[14] D. Dominé et al., Phys. Stat. Sol. (RLL) 2 (2008) 163.
[15] J. Krc et al., J. Appl. Phys. 92 (2002) 749.
[16] P. Buehlmann et al., 22nd EUPVSEC, 2007, p. 2182.